6th European Conference on Computational Mechanics (ECCM 6)
7th European Conference on Computational Fluid Dynamics (ECFD 7)
1115 June 2018, Glasgow, UK

AN EFFICIENT TWO-LAYER WALL MODEL FOR HIGH REYNOLDS NUMBER LARGE EDDY SIMULATION

J. CALAFELL[1], F.X. TRIAS[1] AND A. OLIVA[1]

[1] Heat and Mass Transfer Technological Center, Technical University of Catalonia (UPC)
Colom 11, 08222, Terrassa, Barcelona, Spain.
cttc@cttc.upc.edu

Key words: Wall Modeling, Time Filtering, Two-Layer Model, LES

Abstract. Wall-bounded flows at high Reynolds number are an important research field given that they are present in many important industrial applications. Nonetheless, the use of accurate numerical methodologies such as Large Eddy Simulation (LES) for routine industrial applications, is still unfeasible due to their heavy computational cost. Wall-Modeled LES is intended to circumvent the massive costs of accurately resolving the boundary layer while benefiting from the temporal and spatial resolution of an LES computation. In this work, a Two-Layer Wall Model with a general formulation suitable for non-equilibrium flows and complex geometries is presented. The Two-Layer Models (TLM) suffer from two recurrent problems, the "log-layer mismatch" (LLM) and the resolved Reynolds stresses inflow (RRSI). Until now, complex and expensive techniques have been proposed to overcome these problems separately. In the present work, a time-averaging filter (TAF) is considered to deal with both issues at once, with a single and low-computational-cost technique. It is the first time that the TAF technique is used to block the RRSI. In this regard, a numerical experiment is initially performed to assess the TAF ability in doing so. Afterward, the WM is tested in regular operating conditions with a $Re_\tau \approx 3000$ pipe flow case. Good results are obtained in all the performed tests, showing the capability of the TAF of suppressing the LLM while avoiding the RRSI at the same time. This makes the new TLM methodology a very efficient technique compared to other implementations proposed so far.

1 INTRODUCTION

The modelization of high Reynolds number wall-bounded flows is a relevant research field given the large number of industrial applications in which they are present, among them, wind energy-related and aerospatial devices. However, accurate numerical simulations of this kind of flows are extremely demanding from a computational cost viewpoint. To overcome this difficulty, a vast range of numerical strategies are being developed to make accurate simulations feasible. The present work is focused in wall-modeled Large Eddy Simulation (WMLES), a strategy intended to take advantage of the LES accuracy while minimizing the computational costs derived from the complex near-wall flow

physics. The WMLES approach is based on modeling the boundary layer in one way or another, unlike in the wall-resolved LES (WRLES) technique, in which the boundary layer is explicitly resolved, entailing substantial computational costs.

Several works attempting to estimate the advantages of using WMLES instead of WRLES regarding the grid resolution requirements can be found in the literature. Choi and Moin[1] proposed two expressions for the Reynolds number scaling of the required grid resolution in the wall region. For a WRLES, the number of grid points scales proportionally to $Re_{L_x}^{13/7}$, while for a WMLES, the scaling law is proportional to only Re_{L_x}. However, not only the mesh resolution has effects on the total computational costs. The time step size also plays a crucial role in this aspect since parallelization in time, although it is a current research topic, is of great difficulty.

In the TLM approach, a set of governing equations are numerically resolved in a mesh placed between the solid wall and the first off-wall row of nodes. This mesh is generated by extruding the superficial wall mesh along the wall-normal direction up to the first nodes. The model equations can vary in complexity, from simple equilibrium models in which only the diffusive term of the Unsteady Reynolds-Averaged Navier-Stokes (URANS) equations is taken into account, to accurate models in which the full equations, including all terms, are solved. The present model is based on the latter strategy in order to provide a general formulation applicable to non-equilibrium complex flows.

Despite the apparent advantages of the wall modeling strategy, this approach is not free of problems. A persistent error called "log-layer mismatch" (LLM) is present in most of the WM formulations. According to Cabot and Moin [3] and Kawai and Larsson [4], the LLM is due to the presence of large numerical errors in the near-wall nodes. On the other hand, in the TLM strategy, when the convective term is taken into account in the model physical formulation, a particular source of error called resolved Reynolds stresses inflow (RRSI), also appears [5]. Several strategies have been proposed so far to mitigate the LLM and the RRSI problems [4, 6]. Nevertheless, the proposed methodologies have a significant computational cost and a large degree of implementation complexity making the efficiency of the WM to drop dramatically. Moreover, the LLM and the RRSI problems have always been dealt with separately, forcing the use of at least two computationally expensive measures, one for each issue.

The present strategy is based on applying a time-averaging filter (TAF) to the LES/WM interface. This methodology allows blocking the RRSI while avoiding the LLM problem at the same time, with a single, simple, and low-computational-cost technique boosting the WM efficiency compared to other existing techniques. The TAF technique was firstly introduced by Yang et al. [7] to stabilize the computation of an integral boundary layer wall model by making physically consistent the model input with its mathematical formulation. More recently, Yang et al. [8] reported good results taking the WM input data from the first row of off-wall nodes when using the TAF. According to the authors, the TAF breaks the unphysical temporal synchronization between the LES velocity at the first off-wall nodes and the wall shear stress, which according to the new theory developed in their work, it is the origin of the LLM.

In the present work, the TAF technique is applied to a TLM for the first time. The

primary mission of the TAF is blocking the RRS inflow, being the first time that a TAF is used for this purpose. According to the results presented in sections below, this approach performs significantly better in blocking the RRSI compared to other methods proposed so far [6]. Therefore, taking into account the findings of Yang et al., the TAF suppresses the LLM and the RRSI problems with single step and with a fraction of the computational cost of previously proposed methods[4, 6].

In order to analyze in detail the performance of the TAF in suppressing the RRSI, a numerical experiment based on a pipe flow test at $Re_\tau \approx 500$ will be carried out. Afterward, the wall model (WM) will be tested under regular operating conditions. This will be carried out by computing an equilibrium pipe flow at $Re_\tau \approx 3000$. All tests will be performed in LES-only and WMLES configurations. In case of WMLES, the tests will be carried out with and without TAF. All the obtained numerical results will be compared with DNS from different authors depending on the test [14, 15].

2 Mathematical and numerical method

In this section, the mathematical and numerical methodology of the LES domain and the WM is detailed below.

2.1 LES domain mathematical and numerical strategy

The spatial filtered Navier-Stokes equations are solved numerically within the LES mesh. These equations can be written as,

$$\nabla \cdot \overline{u} = 0, \tag{1}$$

$$\frac{\partial \overline{u}}{\partial t} + (\overline{u} \cdot \nabla)\, \overline{u} + \nabla \overline{p} - \nu \nabla^2 \overline{u} = \nabla \cdot \left(\overline{u}\, \overline{u}^T - \overline{u u^T} \right) \approx -\nabla \cdot \tau(\overline{u}), \tag{2}$$

where $\overline{(\cdot)}$ is the spatial filtering operator, u the velocity field, p the kinematic pressure and $\tau(\overline{u})$ the subgrid stress tensor which is modelled according the Boussinesq hypothesis for incompressible flows:

$$\tau\left(\overline{u}\right) = -2\nu_{sgs} S(\overline{u}), \tag{3}$$

where $S(\overline{u})$ is the rate-of-strain tensor $\left(S(\overline{u}) = \frac{1}{2}\left(\nabla \overline{u} + \nabla \overline{u}^T\right)\right)$ and ν_{sgs} is the subgrid viscosity.

To close the formulation, it is necessary to find an expression for ν_{sgs}. In the present work, two different subgrid strategies will be used, the Wall-adapting local eddy-viscosity (WALE) model of Nicoud [9] et al. for the WRLES computation, and the original Smagorinsky model [10] for the pipe flow test at $Re_\tau \approx 3000$. In the WRLES test, the WALE model will be used since the main purpose of the LES domain is feeding the WM with accurate time-resolved data to analyze the TAF performance. Therefore, an LES model with a reliable behavior in the presence of solid walls is needed. On the other hand, in the WMLES pipe flow test at $Re_\tau \approx 3000$, it is not necessary to have a

good subgrid model performance near the wall since the main purpose is to analyze the improvements introduced by the WM in the global modeling strategy.

Regarding the governing equations discretization, second-order symmetry-preserving schemes are used for the spatial interpolation in a collocated unstructured mesh. Such schemes preserve the symmetry properties of the continuous differential operators ensuring both, the stability and the conservation of the kinetic-energy balance even at high Reynolds numbers and with coarse grids [11]. For the temporal discretization of the momentum equations, a second-order one-step explicit scheme for the convective and diffusive terms[12] is applied, while for the pressure, an implicit first-order scheme has been used. Finally, a fractional-step method is applied to solve the pressure-velocity coupling.

2.2 The Two-Layer model technique

The present TLM strategy is based on the implicit resolution of the full three-dimensional URANS equations (4) in a fine embedded mesh called wall domain mesh (WDM) which stretches from the wall up to the first off-wall row of nodes (see Figure 1).

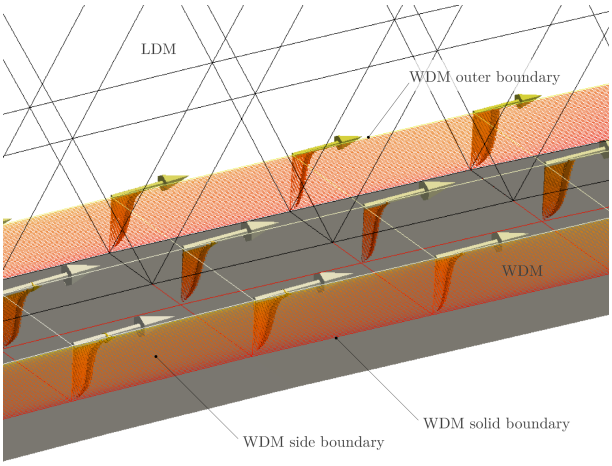

Figure 1: TLM scheme. The WDM is embedded into the LES mesh.

$$\frac{\partial U}{\partial t} + (U \cdot \nabla) U = \nabla \cdot [2(\nu + \nu_{Twm}) S(U)] - \nabla P, \tag{4}$$

where the capital letters stand for time-averaged magnitudes, and ν_{Twm} is the RANS turbulent viscosity for the WM.

The equations are solved numerically through the finite volume methodology. The numerical schemes are the same as those used for the LES domain. To solve the velocity-pressure coupling, an implicit projection method has been implemented [13] to avoid stability restrictions derived from the CFL conditions.

The LES data taken from the first off-wall nodes is used as a boundary condition for the numerical resolution of the equations within the WM layer. Once an accurate near-wall

velocity field has been obtained, it is used to compute a precise wall shear stress which is fed back to the LES domain through the solid boundary faces.

The turbulence model used in the present implementation to evaluate ν_{Twm}, is a mixing-length model which has been applied in most of previous TLM implementations[2, 4, 6] obtaining good results.

$$\nu_{Twm} = \left(\kappa y^+\right)^2 |S| \left[1 - exp\left(-y^+/A^+\right)\right]^2, \tag{5}$$

where $\kappa = 0.41$ is the von Kármán constant, y^+ is the wall distance in wall units, $|S|$ is the magnitude of the rate-of-strain tensor and $A^+ = 26$ is a wall-damping function constant.

In the TLM strategy, different governing equations can be used to model the near wall flow field. In our implementation, the URANS equations, including the advective and pressure terms, have been selected to obtain a general model capable of modelizing unsteady non-equilibrium flows. Nonetheless, the inclusion of the advective term causes the RRSI which has to be corrected.

In our implementation, a time-averaging filter is proposed to avoid the RRSI. The TAF is applied to the LES variables before being used as boundary conditions for the WM. The purpose is to suppress the small-scale resolved turbulent fluctuations while keeping the large-scale motion effects. Additionally, according to Yang et al. [8], the TAF also tackles the LLM problem, allowing to solve the two recurrent problems which affect the Two-Layer models with a single and low-computation-cost step.

An exponential running average method[7] is used for the TAF. This methodology enables to readily prescribe a characteristic averaging time-scale (T) which has to be set to account for the flow large structures effects. Therefore, the averaging period T has to be a fraction of the characteristic time of the simulated flow, for instance, the flow-through period in a pipe or channel flow, or the vortex shedding period in a square cylinder case. The sensitivity of the results to T has been assessed during the validation tests, concluding that it has little influence if T is sufficiently large to filter the RRSI while taking into account the large-scale motion effects.

3 Time-average filter assessment

In this section, the ability of the TAF in blocking the resolved Reynolds stresses inflow will be analyzed. The consequence of the RRSI is an overprediction of the skin friction evaluated by the WM, which is its key output magnitude, preventing the model from providing accurate numerical predictions. A numerical experiment based on a wall-resolved LES (WRLES) of a pipe flow at $Re_\tau \approx 500$ will be performed. The purpose of this experiment is not to evaluate the behavior of the WM in normal operating conditions, but to assess the ability of its mathematical and numerical formulation in reproducing the boundary layer physics within the WM layer. To do so, the WM will be applied to the pipe flow WRLES computation at the height of $y^+ = 40$. The model will be fed with time-resolved LES data but without feeding back the WRLES computation with the WM output. Afterward, the velocity profile within the WM mesh will be compared with DNS data of Chin *et al.*[14] while the computed Re_τ value will be compared with the reference

value of $Re_\tau \approx 500$ as a measure of the ability of the model to evaluate the wall shear stress correctly. This process will be done with and without applying the TAF in order to analyze its effects on the numerical results.

The WRLES computation parameters are as follows: The domain is a pipe of radius R and length $Lx = 8R$, larger than the minimum length of 2π necessary to obtain one-point first and second order converged statistics for a $Re_\tau \approx 500$[14]. Regarding the mesh parameters, a structured mesh is used between $r = 0.5R$ and $r = R$ while between the pipe center and $r = 0.5R$ an unstructured pattern is applied to avoid sharp control volumes at the pipe axis. The total number of grid points of the LES mesh is 6×10^6 with the following distribution: $N_z = 256$, $N_\theta = 192$ and $N_r = 60$ for $r \in [0.5R, 1.0R]$, being z the streamwise, θ the angular and r the radial directions, respectively. The grid spacings in wall units are $\Delta z^+ = 15$, $\Delta r\theta^+ = 1.65$ at $r = R$ and $\Delta r^+ = 1.2$ at the wall. Regarding the WM mesh, it is extruded up to $y^+ = 40$, which is a usual working position for a TLM. It is generated by extruding 10 layers which are concentrated towards the wall, being the first off-wall node well into the linear velocity profile region at a distance of $y_1^+ = 0.36$. Regarding the subgrid strategy, the WALE model is used.

On the other hand, periodic boundary conditions are used in the streamwise direction while non-slip and Neumann conditions are applied at the walls for velocity and pressure, respectively. The flow motion is imposed by requiring a constant mass flow matching the prescribed bulk velocity $\overline{U}$.

Finally, the WRLES computation has been advanced in time during 100 flow-through times until reaching the statistically stationary regime. Afterward, the WM has been coupled to the simulation with no feedback to the LES domain while averaged variables in the wall domain have been collected during 10 flow-through periods.

3.1 TAF assessment test results

In table 1, the Re_τ value computed by the WM is displayed together with its relative error with respect the reference value of $Re_\tau \approx 500$. Two tests have been carried out using the same numerical arrangement, except for the application of the TAF. In case 1, the TAF is not used while in case 2, it is applied to the LES variables.

Table 1: TAF performance assessment test based on a WRLES of a channel flow at $Re_\tau \approx 500$. The computed Re_τ values obtained by the WM with the filtered and non-filtered configurations are shown. The relative error with respect to the reference value ($Re_\tau \approx 500$) also displayed. Symbols are to identify the numerical results in Figure 2

Test	Symb.	TAF	Numerical Re_τ	rel. err. [%]
1	+	no	561.87	12.37
2	∘	yes	504.71	0.94

In figure 2, the mean velocity profiles within the wall model layer obtained with and without using the TAF are displayed.

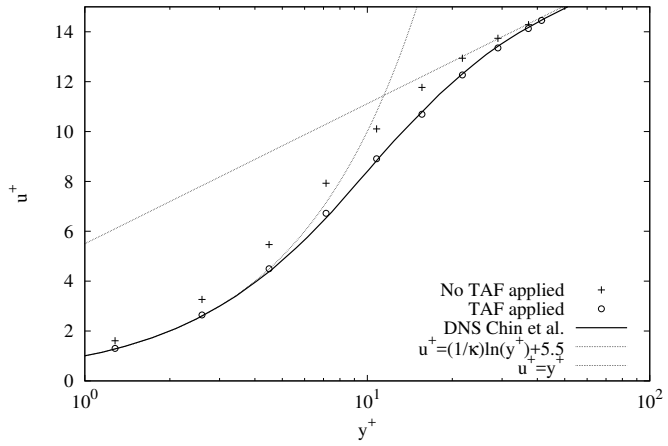

Figure 2: Mean velocity profiles in wall units and logarithmic scale within the WM layer. The results are obtained with and without applying the TAF and compared with DNS data of Chin et al. [14].

The obtained results show that the TAF is able to almost completely suppress the RRSI. According to the results displayed in table 1, the wall shear stress overprediction has been avoided by using the filter. Given that the wall shear stress is a function of the velocity gradient at the wall, the velocity profile has to be correctly evaluated at least in that region. This is confirmed in figure 2, where it can be observed the remarkable improvements caused by the TAF in the mean velocity profile prediction throughout the wall layer. It is worth noting that in this case, the LLM problem is not present and does not distort the results since the LES data is collected far above the first off-wall node [4].

4 Pipe Flow test at $Re_\tau \approx 3000$

In the present test, the WM will be tested under regular operating conditions with an equilibrium pipe flow at $Re_\tau \approx 3000$. Three different configurations will be computed, an LES-only, a non-filtered WMLES, and a filtered WMLES arrangement. This will allow quantifying the improvements introduced by the WM and the TAF by assessing the differences between the numerical results. The setup of the LES domain is the same than in Section 3, but with WMLES grid spacing requirements [1]. Specifically, $\Delta z^+ = 236$, $\Delta r\theta^+ = 198$ at $r = R$ and $\Delta r^+ = 60$, being the first off-wall LES nodes placed at $y_1^+ = 30$, which is the WM/LES interface position. The WM mesh resolution in the wall-normal direction is 10 point with the nodes concentrated towards the wall, being the position of the first off-wall nodes $y^+ \approx 0.1$. Regarding the subgrid strategy, the Smagorinsky model [10] is used.

4.1 Pipe Flow test at $Re_\tau \approx 3000$ results

In table 2, the computed Re_τ value is displayed for the LES-only and the WMLES configurations. In the WMLES test, the results have been obtained using and not using the TAF. The relative error with respect to the reference value which is exactly $Re_\tau = 3026$

is also shown.

Table 2: Computed Re_τ values. The numerical results are obtained with the original Smagorinsky model in three different configurations, LES-only, and WMLES with and without TAF. The relative error in (%) with respect the reference value ($Re_\tau = 3026$) is also displayed.

Test	TAF	Numerical Re_τ	rel. err. [%]
LES-only	N/A	954.1	68.4
WMLES	no	3381.4	11.74
WMLES	yes	3155.6	4.20

In figure 3, the mean velocity profiles in the streamwise direction for the three configurations are shown. The results are compared with the DNS data of Ahn et al. [15] and the law of the wall. On the other hand, in figure 4, the root mean square (rms) velocity fluctuations obtained in the same conditions than the previous plot, are displayed. The results are provided for the three spatial directions (u'^+, v'^+ and w'^+) as well as the Reynolds shear stress (uv'^+). In all plots, all data is given in wall units except for the wall distance in the velocity fluctuation charts.

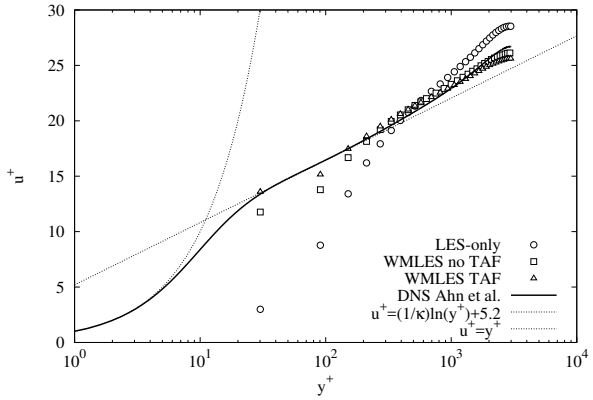

Figure 3: Mean velocity profiles in the streamwise direction of the LES domain in wall units and logarithmic scale. The numerical results are obtained with the original Smagorinsky model in three different configurations, LES-only, and WMLES with and without TAF. The obtained data is compared with the DNS of Ahn et al. [15].

The results of the computed Re_τ displayed in table 2 show a significant improvement in the wall shear stress evaluation when using the WM, from a relative error of 68.4% in the LES-only test to a 4.2% in the time-filtered WMLES case. According to these results, the TAF is performing well regarding the RRSI blocking efficiency, reducing the wall shear stress overprediction from 11.74% in the WMLES without TAF to 4.20% in the filtered solution. Regarding the mean velocity profiles, an important improvement is observed when using the WM with respect to the LES-only test. This is an expected outcome

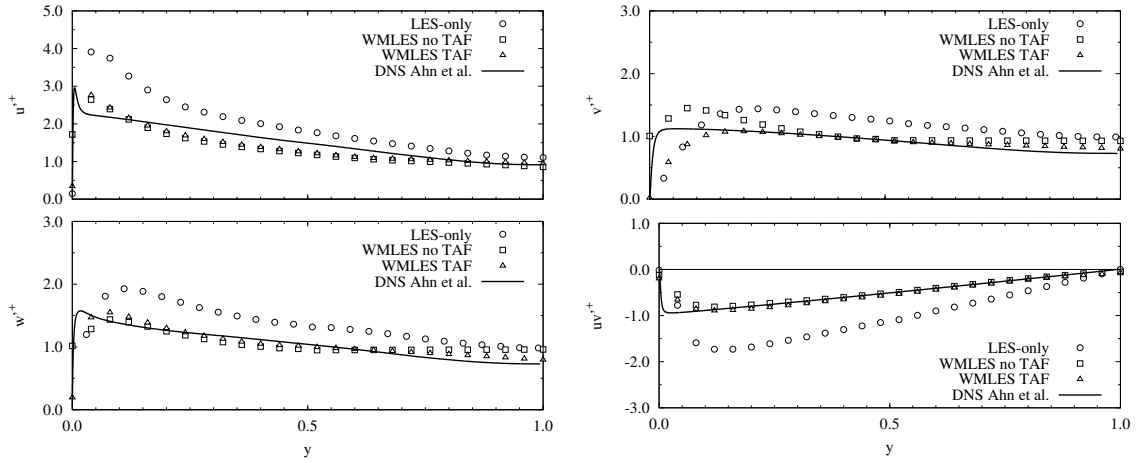

Figure 4: Rms velocity fluctuation profiles in the three directions directions (u'^+, v'^+ and w'^+) as well as the Reynolds shear stress (uv'^+) in the LES domain. The numerical results are obtained with the original Smagorinsky model in three different configurations, LES-only, and WMLES with and without TAF. The obtained data is compared with the DNS of Ahn et al. [15].

since the original Smagorinsky subgrid model has a poor near-wall behavior. However, a significant improvement is subsequently obtained by applying the TAF. This enhancement is due to two overlapped effects of the TAF. On the one hand, the block of the RRSI, and on the other hand, the elimination of the LLM problem, an effect pointed out by Yang et al. in a recent publication [8]. Finally, concerning the rms velocity fluctuations, an improvement is also obtained with the use of the WM, especially when the TAF is applied. However, this is only true for the pipe's core region. In the near-wall area, the numerical predictions are rather poor. This is due to the high ratio between the flow structures size and the grid resolution in this area. The size of the eddies is proportional to the wall distance, and therefore, with a constant grid spacing, the mesh resolution is especially poor in the near-wall region, an effect which the WM cannot counterbalance.

5 Conclusions

The time-average filtering (TAF) technique is used for the first time in the TLM context. This approach allows to tackle two recurrent problems in TLM; the resolved Reynolds stresses inflow (RRSI) and the "log-layer mismatch" (LLM) issues. In this sense, it is the first time that a TAF is used to block the RRSI, while the effects on the LLM, were recently published by Yang et al. [8]. In the present work, an initial numerical test based on a WRLES pipe flow at $Re_\tau \approx 500$ is used to assess the performance of the TAF in avoiding the RRSI. Afterward, the strategy is tested according to the WM standard operating conditions with a pipe flow at $Re_\tau \approx 3000$. According to the obtained numerical results, the TAF is able to almost completely block the RRSI while avoiding the LLM with a single and low-computational-cost step. This makes the present implementation a highly efficient strategy if compared with existing methodologies proposed so far [4, 6].

6 Acknowledgements

This work has been financially supported by Ministerio de Economa, Industria y Competitividad, Spain (ENE2017-88697-R).

REFERENCES

[1] Choi, H. and Moin, P. Grid-point requirements for large eddy simulation: Chapman's estimates revisited. *Phys. Fluids* (2012) **24**:011702

[2] Balaras, E. and Benocci, C. and Piomelli, U. Two-Layer Approximate Boundary Conditions for Large-Eddy Simulations. *AIAA J.* (1996) **34(6)**:1111–1119

[3] Cabot, W. and Moin, P. Approximate Wall Boundary Conditions in the Large-Eddy Simulation of High Reynolds Number Flow. *Flow Turbul. Combust.* (1999) **63**:269–291

[4] Kawai, S. and Larsson, J. Wall-modeling in large eddy simulation: Length scales, grid resolution, and accuracy. *Phys. Fluids* (2012) **24**:015105

[5] Cabot, W. Near-wall models in large-eddy simulations of flow behind a backward-facing step. *Annual Research Brief. Center for Turbulence Research, Stanford, CA.* (1999) 199–210

[6] Park, G. I. and Moin, P. An improved dynamic non-equilibrium wall-model for large eddy simulation. *Phys. Fluids* (2014) **26**:015108

[7] Yang, X. I. A. and Sadique, J. and Mittal, R. and Meneveau, C. Integral wall model for large eddy simulations of wall-bounded turbulent flows. *Phys. Fluids* (2015) **27**:025112

[8] Yang, X. I. A. and Park, G. I. and Moin, P. Log-layer mismatch and modeling of the fluctuating wall stress in wall-modeled large-eddy simulations. *Phys. Rev. Fluids* (2017) **2**:104601

[9] Nicoud, F. and Ducros, F. Subgrid-scale stress modeling based on the square of the velocity gradient tensor. *Flow. Turbul. combust.* (1999) **62**:183–200

[10] Smagorinsky, J. General circulation experiments with the primitive equations, I. The basic experiment. *Monthly Weather Review* (1963) **91**:99–164

[11] Verstappen, R. W. C. P. and Veldman, A. E. P. Symmetry-preserving Discretization of Turbulent Flow. *J. Comput. Phys.* (2003) **187**:343–368

[12] Trias, F. X. and Lehmkuhl, O. A self-adaptive strategy for the time-integration of NavierStokes equations. *Numer. Heat Tr. B-Fund.* (2011) **60-2**:116–134

[13] Carmona, A. and Lehmkuhl, O. and Pérez-Segarra, C. D. and Oliva, A. Numerical analysis of the transpose diffusive term for viscoplastic-type non-Newtonian fluid flows using a collocated variable arrangement. *Numer. Heat Tr. B-Fund.* (2015) **67**:410–436

[14] Chin, C. and Ooi, A. S. H. and Marusic, I. and Blackburn, H. M. The influence of pipe length on turbulence statistics computed from direct numerical simulation data. *Phys. Fluids* (2010) **22**:115107

[15] Ahn, J. and Lee, J. H. and Lee, J. and Kang, J. H. and Sung, H. J. Direct numerical simulation of a 30R long turbulent pipe flow at $\mathrm{Re}_\tau = 3008$. *Phys. Fluids* (2015) **27**:065110